PHOTONS TRANSMISSION FACTORS FOR GRANITE AND POLYBORON LAMINATED CONCRETE WALLS

Oche, C. O.,[1] Olarinoye, I. O.[1] and Ahmadu, U.[1]
[1]*Federal University of Technology, Minna Niger State*
*Corresponding author email: Ochegabasphysics@gmail.com

ABSTRACT

In the present study, the photon exposure transmission factors (TF) of granites, concrete plaster paste, concrete, Polyboron (PB) together with granite (GPC_160) and Polyboron (C+PB) laminated concrete wall structures is presented for photons in therapeutic energy range (15keV to 3MeV). The TF were calculated using values of mass attenuation coefficients (MAC) and exposure buildup factors for the six materials using WinXCom and EXABCal computer codes respectively. The Transmission factors and their variations with photon energy and thickness of materials have been discussed. The obtained result showed that MAC, LAC and mfp strongly depends on the photon energy, chemical composition and density of the shielding materials and thus for single materials, plaster had the highest value of MAC across the energies due to its high Zeq across the energies. Furthermore, due to its relatively lower Transmission factor, GPC_160 attenuates photons better than the conventional concrete and Polyboron laminated walls for the considered energy range..

Keywords: Buildup factor, EXABCal, Granite, Shielding, Exposure transmission factor, Polyboron.

1.0 INTRODUCTION

Ionizing radiations (IR) have applications in medicine (for diagnosis and therapeutic purposes); environmental conservation; agriculture and food processing; archeological and cultural preservation; radio-tracing in industries; ultrasonic crack verifications in metallic industries; and electricity production via nuclear reactors [1-6]. Despite the benefits derived from these applications, uncontrolled exposure of man and the non-human biota to IR could be hazardous depending on the level of exposure. Over exposure of ionizing radiation could result from procedural or unregulated applications of radiation and nuclear accidents. However, the exposure could be made low through the use of structural shield. Buildings where radiation facilities are to be operated require special architectural design to provide protection against unsolicited radiation exposure beyond the buildings. Materials with good shielding parameters must be considered for such construction depending on the dose allowed outside the shield and the radiation of interest. cases there may be need to convert existing ordinary building to radiographic centre with Radiography/Radiotherapy room or an equipment repository room for rig workers on an emergency or temporal basis. Such buildings require extra shielding provision since the original function was not for radiation application. In another case emergency shelter with good shielding capacity may be required during nuclear accidents. The wall of such structure may be laminated with suitable materials to provide adequate shielding as may be required without having to pull down and reconstruct such buildings.

One of the ways to improve the shielding capacity of existing structures is to laminate their walls with a material having superior shielding parameters.

In recent years the photon interaction coefficients of structural materials such as clay, marbles, desert sand, granites, Polyboron, concrete, pure polyethylene, borated polyethylene have been investigated [12-18].

In the present, work we evaluate the photon transfer factors (TF) of granite, Polyboron (PB), ordinary concrete, granite and PB laminated walls. The TF were calculated from their respective mass attenuation coefficients and exposure buildup factors for photon energies between 15 keV and 3 MeV.

Theory on the Study

2.1 Mass Attenuation Coefficient

When a beam of monochromatic photons is incident on a thin absorbing medium of mass thickness t, the intensity is reduced on emerging from the medium according to the equation:

$$I = I_o e^{-\mu_m t} \quad (1)$$

Where I, I_o and μ_m are respectively the transmitted (attenuated), incident photon densities and the mass

attenuation coefficient of the material medium. The μ_m measures the mean number of photo-interactions between the incident photons and the absorbing medium at a given mass thickness. The $\mu_m$can be used to compare the photon shielding capacity of different material at specific photon energy. It is experimentally determined using equation 1 or theoretically through the use of computer codes such as MCNP5 and XCOM [21, 22]. For composite material, the $\mu_m$is estimated using the mixture rule from the equation [23]:

$$\mu_m^c = \sum_i^n w_i \mu_m^i \quad (2)$$

Whereμ_m^c, μ_m^i and w_i are the mass attenuation coefficients of the composite material, the i[th] component in the material and the weight fraction of the i[th] component of the composite material respectively.

2.2 Exposure Buildup Factor

For many practical applications, radiation shields are not thin and photons may not be monochromatic and collimated, consequently, equation 1 is always modified to account for multiple photon scattering and buildup in the thick absorber. The buildup factor (B) accounts for the ratio of broad beam to that of collimated beam and directly influences radiation absorption for absorbed dose or shielding calculations. Generally, the evaluation of buildup factors using the Geometric Progression (G.P) method requires three distinct procedures:

i. Equivalent Atomic Number

To do this for any material, the Compton partial interaction coefficient (μ_c) and mass attenuation coefficients (μ_m) is calculated for the photon energy range 0.015 MeV-15 MeV using the XCOM software. The ratio $R = {}^{\mu_C}/_{\mu_m}$ of each material is then calculated and matched at the standard energies to the corresponding ratios of elements up to the heaviest element. If the value of the radio matches any of the elements', then the atomic number of that element becomes the equivalent atomic number of the material. However, if the value of R obtained for the considered material does not match that of any element but rather falls between the ratios for two successive elements then, the Z_{eq} of such material is interpolated using the expression [21, 27-29]:

$$Z_{eq} = \frac{Z_1(\log R_2 - \log R) + Z_2(\log R - \log R_1)}{\log R_2 - \log R_1} \quad (3)$$

Where, R1 and R2 are the ratios (${}^{\mu_C}/_{\mu_m}$) of the two successive elements of atomic numbers Z_1 and Z_2 respectively within which R falls at each energy.

2.4 Evaluation of GP fitting parameters

Five (5) fitting parameters are required for the evaluation of photon buildup factors by the GP fitting method [27, 28]. These parameters (b, c, a, Xk, and d) depend on Z_{eq} and photon energy. The GP fitting coefficients of the material is also interpolated using the logarithmic interpolation formula:

$$P = \frac{P_1(\log Z_2 - \log Z_{eq}) + P_2(\log Z_{eq} - \log Z_1)}{\log Z_2 - \log Z_1} \quad (4)$$

Where P_1 and P_2 are the G-P fitting parameters obtained from ANS data base corresponding to the atomic numbers Z_1 and Z_2 respectively.

2.5 Estimation of Exposure buildup factor

The exposure buildup factors ($EBF(E,x)$) for a given material is then estimated from the fitting parameters for a given incident energy (E) in the spectrum (0.015 MeV -15 MeV) for different penetration depth (x) up to 40 mfp by the equations [27, 28]:

$$EBF(E,x) = 1 + \frac{(b-1)(K^x - 1)}{K-1} \quad (5)$$

$$EBF(E,x) = 1 + (b-1)x, \quad \text{for } K = 1 \quad (6)$$

$$K(E,x) = cx^a + d\frac{\tanh\left({}^{x}/_{X_K} - 2\right) - \tanh(-2)}{1 - \tanh(-2)} \quad (7)$$

$$\text{for } x \leq 40\ mfp$$

2.6 Transmission Factor

This is a ratio which defines the how much an incident photon of intensity (Io) beam is attenuated or reduced to an intensity (I) after passing through a shield of thickness x and LAC (μ)

$$TF = \frac{I}{I_o} = e^{-\mu x} \quad (8)$$

for most practical purposes the buildup factor correction to the equation as shown in equation 6 is required.

$$TF' = \frac{I'}{I_o} = Be^{-\mu x} \quad (9)$$

2.7 Methodology

Concrete blocks (C) were produced with design mix of cement, fine aggregates, coarse aggregates in the ratio 1:2:3 respectively and a water to cement (w/c) ratio of 0.5. Granite rocks (G) were locally sourced from Bosso area of Minna in Niger State. Similarly, plaster (P) (comprising of Portland cement and Fine aggregates (FA)) was prepared and sundried. After drying the samples were crushed, sieved and packaged for

chemical analysis. The elemental composition of the samples was determined using Energy Dispersive X-ray Fluorescence (EDXRF) spectrometric analysis.

Two wall configurations composed of Graphite (50mm thick) attached to solid concrete block (160mm thick) with plaster (20mm thick) (GPC_160) and Polyboron sheets laminated on the concrete block (C+PB) were constructed as depicted in Figure 1. The proportions by weight and bulk densities of the composite in the wall configurations are shown in Table 1.

The mass attenuation coefficients of C, G, PB, GPC_160 and C+PB were calculated using WinXCOM [23] where the chemical composition of the materials obtained from EDXRF analysis serves as the input parameters. The elemental composition of Polyboron was obtained from literature [11]. To calculate the exposure buildup factors of the materials the EXABCal computer code [24] was used. The results of the mass attenuation coefficients and the buildup factors were then used to evaluate the TF of the wall configurations according to equations 8 and 9.

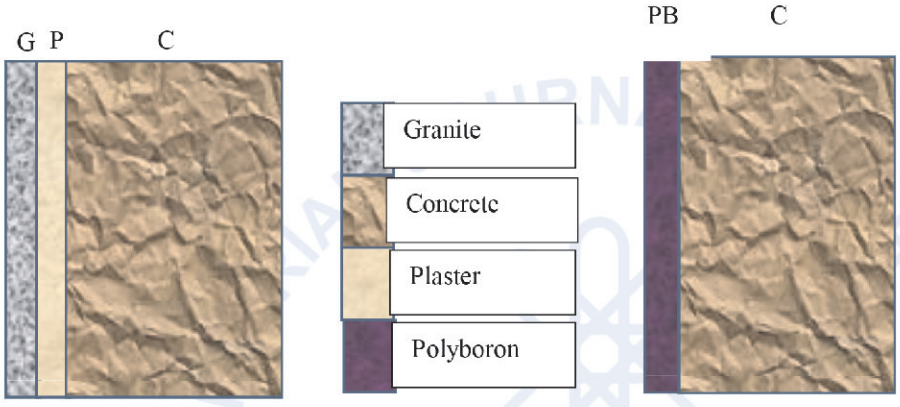

Figure 1: Wall configurations of (a) GPC_160 side view (b) C+PB side view

Table 1: Weight fraction of the different wall components

Configuration	Density (g/cm^3)	Weight Fractions			
		G	P	C	PB
GPC_160	2.34	0.24	0.06	0.7	----
C+PB	1.896	-----	------	0.84	0.16

3.0 RESULTS AND DISCUSSION

The concentration of major and trace elements in C, P, and G obtained from the EDXRF analysis is presented in Table 2 together with that of PB which was obtained from literature [11]. The result show the major elements in C, P, and G to be O, Si, Al.

3.1 Mass Attenuation Coefficient

The values of the mass attenuation coefficient (MAC) μ_m (cm^2/g) calculated with WinXcom for the considered materials comprising of four single materials for energies ranging from 15 keV to 3 MeV and their variation with energy is shown in Figure 2. From the figure, the MAC decreases rapidly with increasing energy up to an energy of 0.1 MeV for all the materials. Beyond this energy, the rate of decrease becomes smaller with increasing energy. The initial rapid decrease is attributed to the dominance of the photoelectric interaction (τ) coefficient at these energies. The τ is proportional to $\frac{Z^5}{E^3}$[21]. This also explains why the high atomic materials C, G and P have higher MAC compare to polyboron that consists of low atomic number constituents. Beyond photon energy of 0.1 MeV, the MAC of the studied material becomes fairly constant due to the dominance of the incoherent scattering (Compton scattering- σ) coefficient. The σ depends on the number of available electrons per unit mass of a material $\left(N_e \propto \frac{Z}{A}\right)$. Since $N_e$is constant for all materials except hydrogen, this explains why the MAC of the materials were almost constant in the Compton interaction dominating region of the energy spectrum. Beyond energy of 10 MeV the dominance of the pair

production interaction mode begins to set in and dictate the behavior of MAC. Since the coefficient of pair production coefficient is proportional to materials atomic number, higher Z materials will have relatively higher MAC as shown in Figure 2.

3.2 Exposure Buildup Factor (EBF)

Figure 3 (a-d) shows the variation of exposure buildup factors for selected single materials at mean free paths 5, 10, 15, 20, 25 and 30. The general trend is consistent across all samples as explained for Figure 2. It can be seen that the lowest buildup is seen in 5mfp while the largest buildup occurs at 30mfp for each of the sample. This is because buildup factor is a function of both energy and depth. The larger the depth of a material, the more mean free paths possible and thus by implication, more buildup possible especially in the range of energy dominated by Compton scattering. In Figure 3c, the photoelectric effect dominated region shows very little prominence as the Compton scattering sets in almost immediately. Furthermore, Polyboron has the largest buildup factors in relation to the remaining materials which is probably due to its low Z_{eq} since high Z_{eq} materials have a higher potential of removing photons by absorption [26] while for the same reason, plaster (high Z_{eq}) has the lowest buildup factor which can lead to the conclusion that Z_{eq} is inversely proportional to the buildup factor at these considered depths.

Table 2: Elemental Composition of granite, plaster, concrete, polyboron and their densities

Element	Plaster (1.52)	Concrete (2.35)	Granite (2.63)	Polyboron (0.971)
H	------	------	------	12.38
C	------	------	------	59.88
O	46.8	49.8	46.26	22.85
Na	------	1.71	1.703	------
Mg	0.6	0.26	0.24	------
Al	6.2	4.57	0.53	------
Si	30.1	31.51	32.71	------
P	------	------	0.044	------
S	------	0.13	------	------
K	------	1.92	1.743	------
Ca	11.4	8.27	1.349	------
Ti	------	------	0.12	------
Mn	------	------	0.077	------
Fe	4.9	1.23	2.45	------
B	-----	-----	------	4.89

3.3 Transmission Factor

The transmission factor of granite, concrete, plaster and Polyboron as single materials evaluated using equation 8 showed varying with thickness (Figure 4 (a-c)). The thicknesses used ranged from 5 to 30cm while the energies considered are 0.2, 0.4 and 0.6MeVs. The trend shows a sharp decrease with the increase in thickness of materials and seeing that transmission factor depends on both the energy of the incident photon and the shield thickness, the trend is as expected. Moving across from a to c, there is an increase in the transmission factor as the energy increases. Across all trends, the transmission factor follow the order:

Granite< Concrete < Plaster < Polyboron

Consequently, the shielding effectiveness across these energies also follow that order with Granite being the better photon shield while Polyboron being the least viable shield. These may be tied to the differences in particle densities of these materials as the higher particle density material means more collision probability rate and hence less transmission. The buildup factor correction of transmission factors is usually used to adapt ideal situations with the real life applications in which case, there is usually some amount of buildups. Thus using equation 9, the Exposure transmission factors of the afore-listed materials have been ascertained and plotted for these same thicknesses (Figure 5). The energies considered are 0.6MeV, 1Mev, 2MeV and 3.0MeV. The exposure transmission factors showed a less sharp decrease with thickness especially for concrete, granites and plaster while Polyboron shows a rather linear decrease with thickness for the chosen energies except for 0.6MeV.

Figure 6 shows the Exposure Buildup factors of three materials (two composite and one single). Buildup factors changes generally in the same trend with energy regardless of the material type or depth being considered. In a general sense, they are lower at lower and higher energies but rise and attains peaks at intermediate energies [21]. These peaks vary with material and penetration depth in consideration across any energy spectrum. This behavior can be understood best using the three interaction modes which are known

to show dominance at different energy range. The spectrum is divided into the lower, intermediate and the higher energy level dominated by the photoelectric, Compton and pair production interactions respectively. At low energies, the photoelectric effect removes the photons from the incident beam thereby preventing buildup. Higher Zeq materials have more likelihood to remove more photons at these energies. This explains the lower BF experienced for concretes as compared to GPC and CB as this energy range. The Overlap experienced at this region can be attributed to the approximately equal values of Zeq for both GPC and C+PB. Furthermore, as the energy increases, the buildup is seen to increase and mounting into a peak. This increase of buildup is due to the fact that during Compton scattering, there is simply multiple scattering and no complete/direct absorption of these photons. Beyond this energy (1.022MeV), the buildup starts to decrease and become low because the pair production at this range removes completely the photons from the incoming beam [21].

Figure 7 (a-c) shows the transmission factor of GPC_160, Concrete and C+PB corrected with buildup factor. This correction avails for a more real life scenario (Bad Geometry). It can be inferred from these figures that an underestimation of the transmission factor would simply result if photon buildup is not considered. The graphs show a sharp rise (high slope) towards an optima then an almost steady progression as it curves rightwards with the uncorrected values lower than those corrected with exposure buildup factor. There is an increase in transmission as the energy of the incident photons is increased. At lower and higher energies, the buildup shows very little effect because at these energies, the buildup of photons is very low owing to the high absorption from both Photoelectric effect and pair absorptions respectively. This that at higher energy, the values for both corrected and uncorrected transmission factors approaching a meeting point. At the intermediate energies, the gap between the corrected and uncorrected transmission values is due to the large buildup factor accumulation from Compton Effect. Figure 8 shows the comparison between the shielding capacities of ordinary concrete, GPC_160 and CB. As shown by equation (8), the transmission factor being dependent on both energy of incident photon and thickness of a material shield is usually low at lower energies and increases with energy increase due to more penetration of such shields. Thus a shield with less transmission ultimately represents a better shield and in this case, GPC_160 has the least transmission factor to about 2.0MeV where CB dropped in its transmission factor below that of concrete and GPC_160.

Table 3.0: Zeq Data for some selected materials

ENERGY	GPC160	C+PB	CONCRETE	PLASTER	GRANITE	PB
1.50E-02	12.88	12.14	12.86	14.01	12.63	6.12
2.00E-02	13	12.28	12.97	14.17	12.74	6.15
3.00E-02	13.12	12.43	13.1	14.36	12.87	6.18
4.00E-02	13.21	12.52	13.18	14.46	12.96	6.19
5.00E-02	13.28	12.59	13.24	14.54	13.03	6.19
6.00E-02	13.32	12.64	13.29	14.6	13.07	6.2
8.00E-02	13.38	12.7	13.34	14.69	13.14	6.2
1.00E-01	13.44	12.75	13.38	14.75	13.18	6.21
1.50E-01	13.53	12.83	13.45	14.85	13.25	6.21
2.00E-01	13.59	12.87	13.48	14.92	13.29	6.22
3.00E-01	13.77	12.93	13.53	15.15	13.34	6.22
4.00E-01	13.34	12.96	13.55	15.26	13.37	6.22
5.00E-01	13.75	12.97	13.57	15.3	13.39	6.22
6.00E-01	12.71	12.98	13.58	15.24	13.39	6.23
8.00E-01	14.68	12.939	13.58	14.68	13.4	6.23
1.00E+00	16.16	12.99	13.58	16.16	13.4	6.23
1.50E+00	11.03	11.05	12.09	13.95	11.88	5.31
2.00E+00	11.58	10.64	11.72	12.38	11.51	5.28
3.00E+00	11.61	10.55	11.63	12.35	11.43	5.28

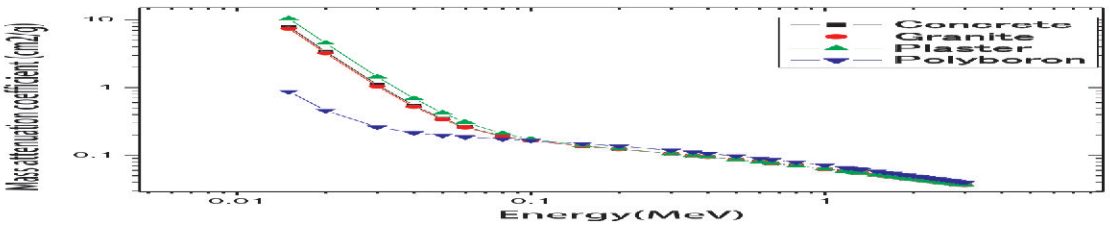

Figure 2: Mass Attenuation Coefficient of Various Materials

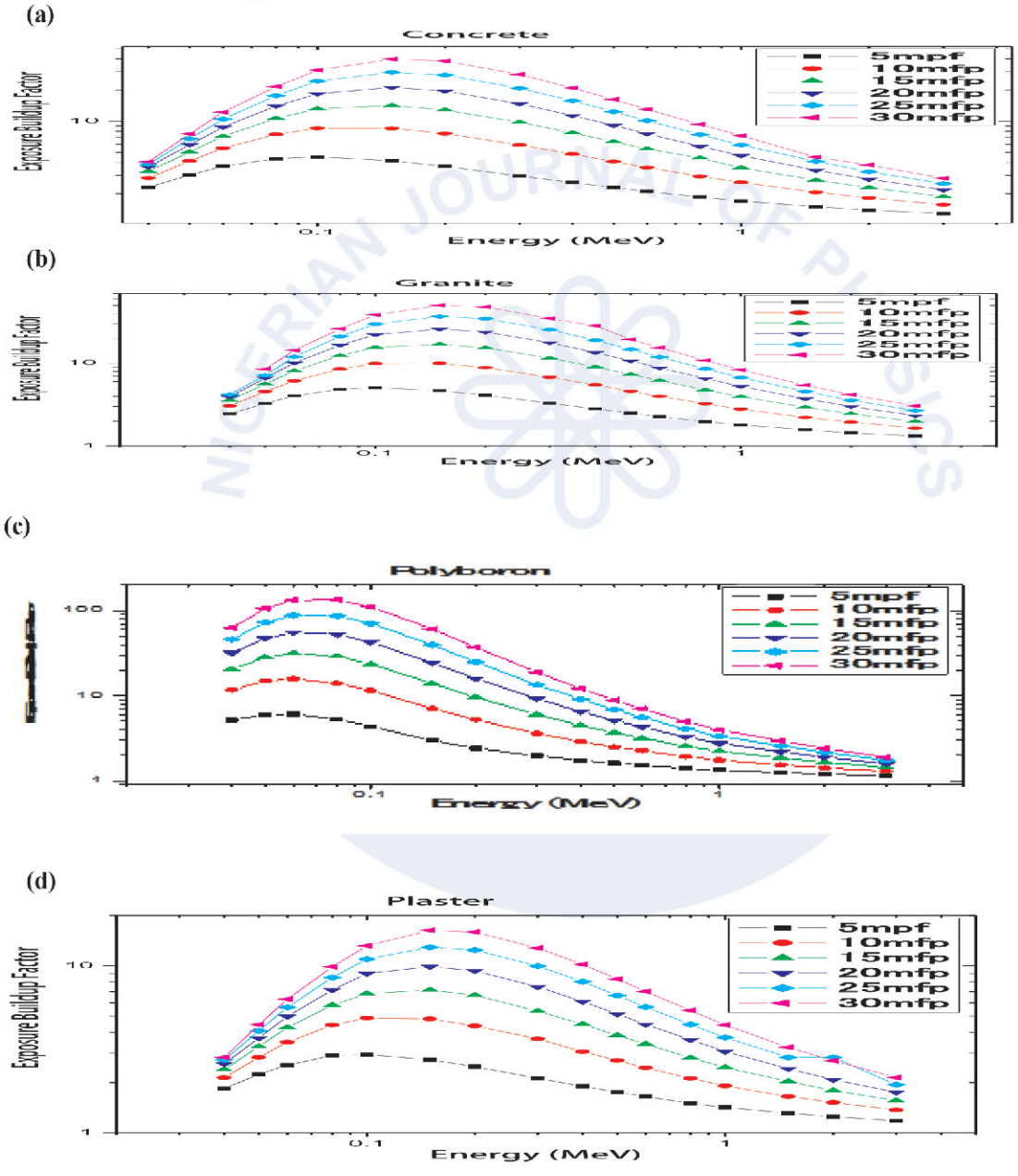

Figure 3 (a-d): Exposure Buildup factors of single materials

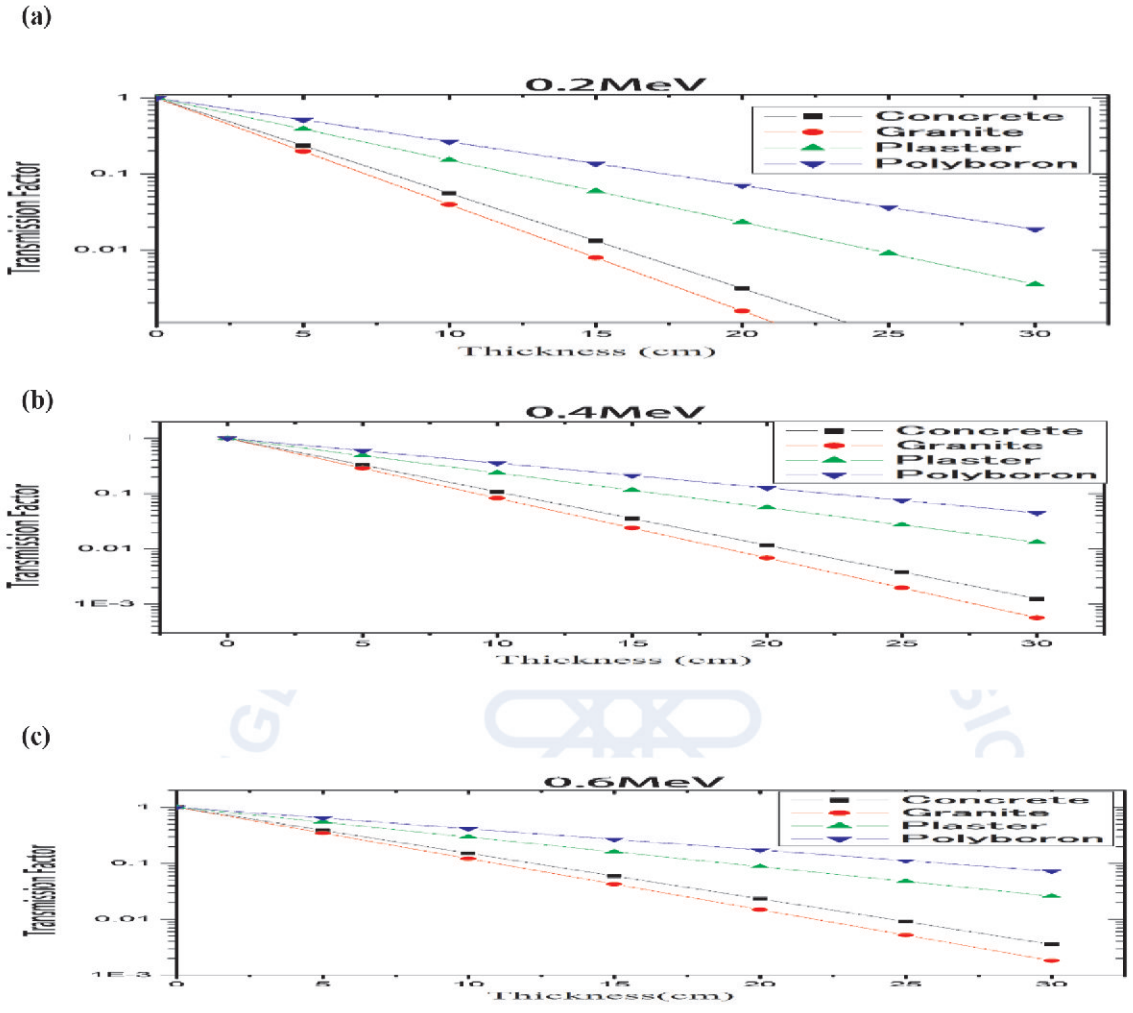

Figure 4: Transmission factors of single materials given at (a) 0.2MeV (b) 0.4MeV (c) 0.6MeV

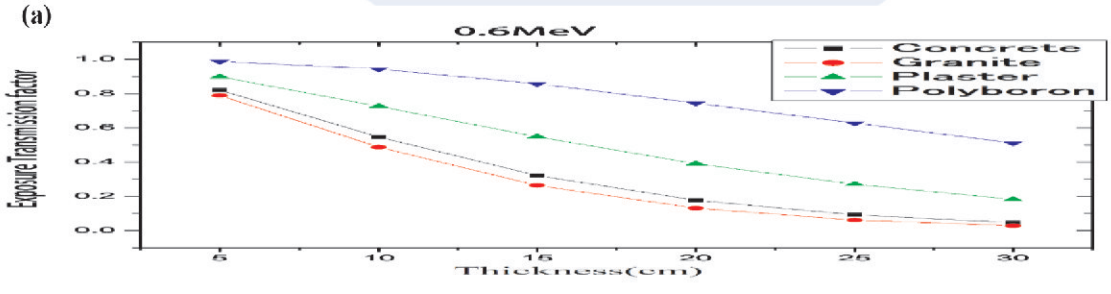

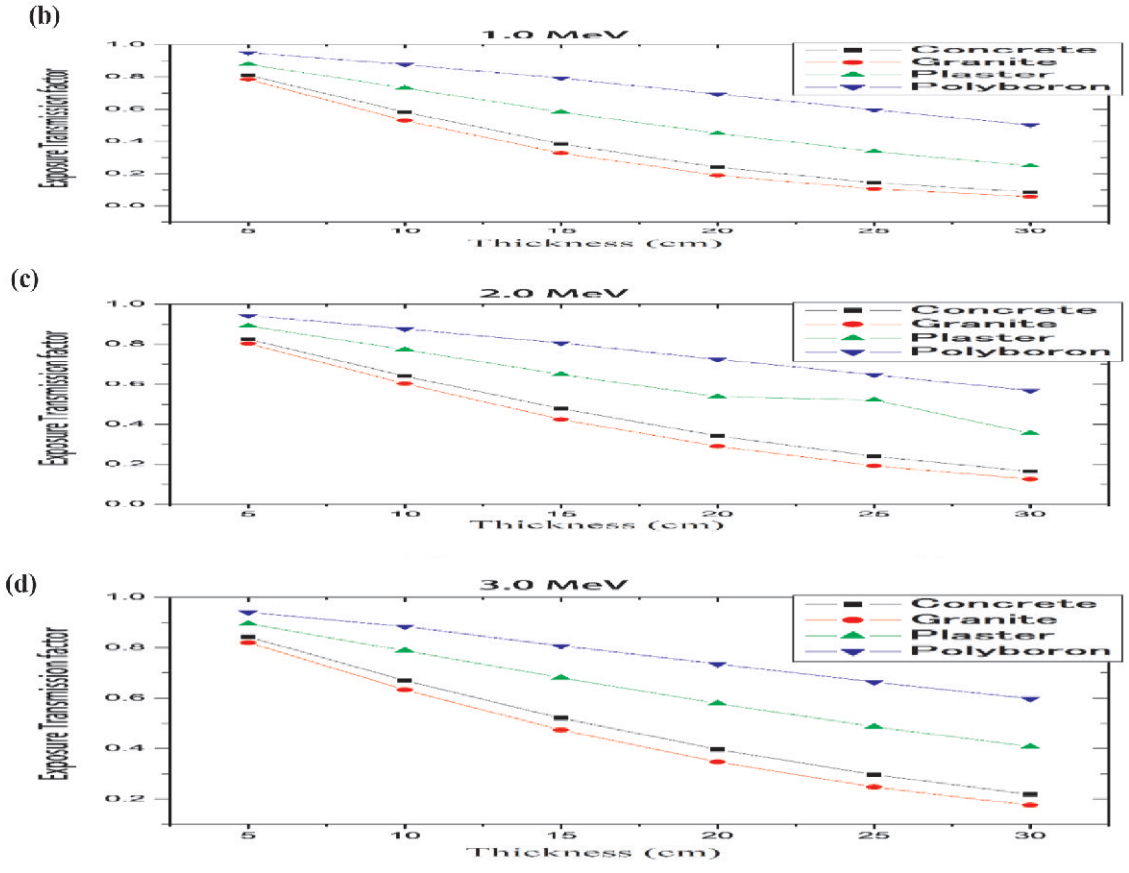

Figure 5: Corrected transmission factors for single materials at (a) 0.6MeV (b) 1.0MeV (c) 2.0MeV (d) 3.0MeV

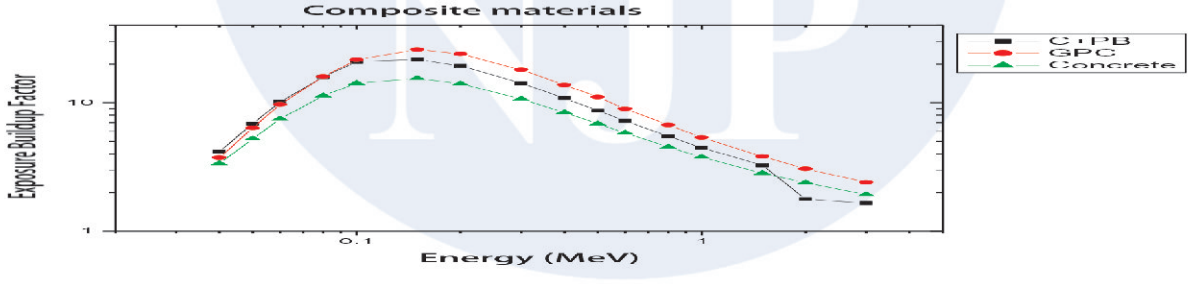

Figure 6: Exposure Buildup factors of various composite walls and concrete

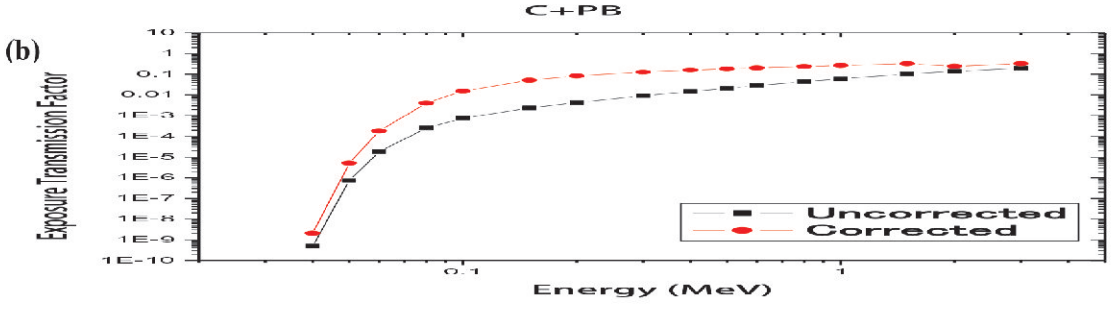

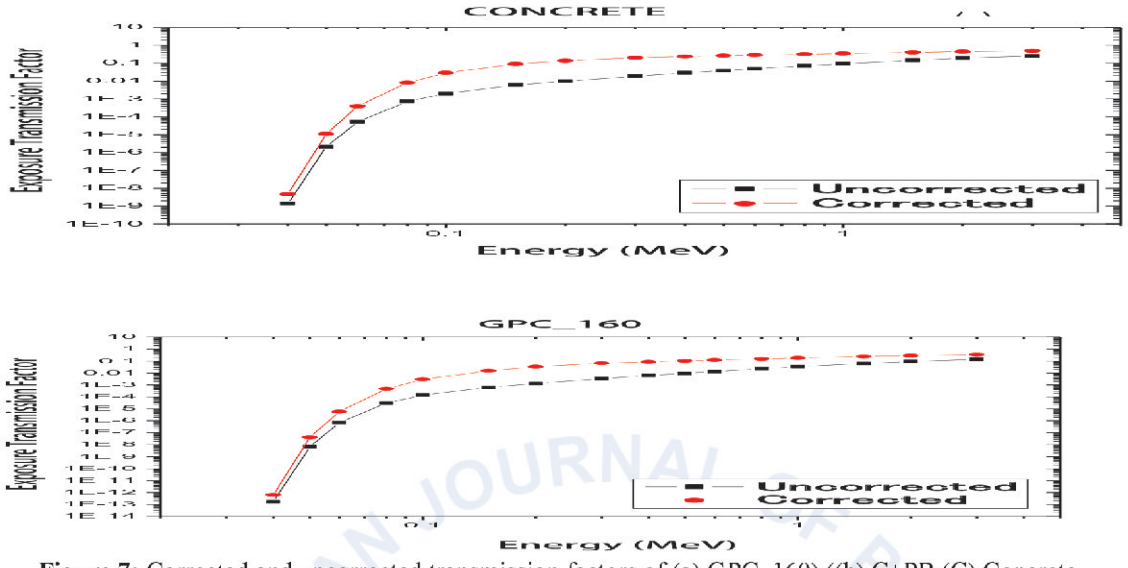

Figure 7: Corrected and uncorrected transmission factors of (a) GPC_160) ((b) C+PB (C) Concrete

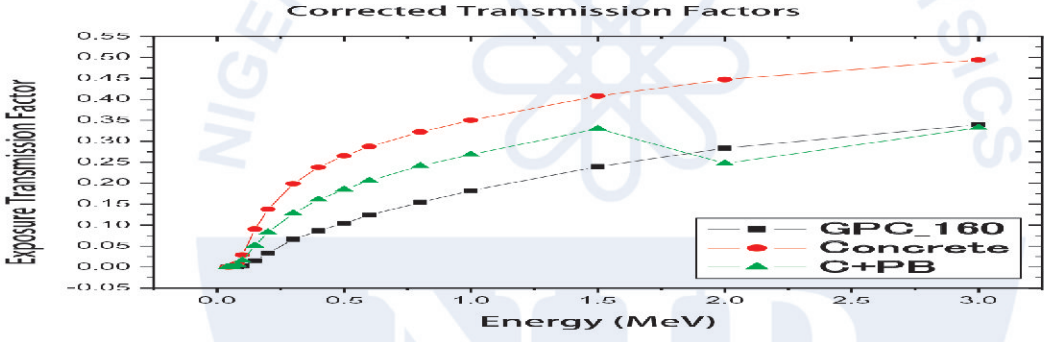

Figure 8: Corrected transmission factors for composite walls and concrete

CONCLUSION

The mass attenuation coefficient, equivalent atomic number (Zeq), exposure buildup factor and transmission factors of single materials (concrete, granite, plaster, Polyboron) and composite wall structures (GPC_160 and C+PB) were calculated for photon energies in the therapeutic range and comparisons have been made between two new wall structures and the conventional concretes. Result shows that the photon shielding capacity of GPC_160 was better than that of ordinary concrete and Polyboron laminated wall (C+PB) on the basis of a clear distinction between their exposure buildup factors corrected transmission factors. Consequently, it can be concluded that for the emergency conversion of facilities into radiotherapy rooms, under-shielded existing radiation facilities or production of shielding for rooms holding sources or activated drilling equipment's repositories, this wall configuration can be used.

REFERENCES

Andrzej, G.C. (2005). Application of Ionizing radiation to environmental protection, *Nucleonika,* 50(3): 17-24.

Balwinder, S., Jaspreet, S., Amritpal, K. (2013). Application of Radioisotopes in agriculture; *IJBBR,* Vol 4 (3): 167-174.

Cancl Eke, Osman Agar, Christian Segebade and Ismail Boztosun (2017). Attenuation properties of radiation shielding materials such as granite and marble against γ-ray energies between 80 and 1350 keV, *Radiochim, Acta*, 1-13.

Christopher, T M. (2017). Evaluation of use of industrial radiography for weld joints inspection in Tanzania, *IJMET,* 65-74.

El-Enany, N. (1998). Study Of Gamma-Ray Shielding Properties Of Desert Sand And Granite Rocks. *Intern. J. Environmental Studies*, 1998, Vol. 55,

pp. 121-128.

Falah, Abu-Jarad (2009). The application of radiation sources in the oil and gas industry and shortages in their services; Atoms for Peace. *An International Journal,* Vol. 2, No. 4.

Harima, Y. (1983). A historical review and current status of buildup factor calculations and applications. *Radiation Physics and Chemistry*, 41: 631-672.

Harima, Y., Sakamoto, Y., Tanaka, S., Kawai, M. (1986). Validity of the geometric progression formula in approximating gamma ray buildup factors. *Nucl. Sci. Eng.*, 94, 24-35.

Hossaini, M.S., Islma, M.A.S., Quasem, M.A. and Zaman, M.A. (2010). Study of shielding behavior of some multilayer shields containing PB and PX. *Indian Journal of Pure and applied Physics,* Vol. 48, 860-868. http://dx.doi.org/10.4236/detection.2016.42005

IAEA (2017). Uses of Ionizing Radiation for tangible cultural heritage conservation, (6).

Ibrahim A. F. (2017). Investigation of gamma ray shielding effectiveness of natural marble used for external wall cladding in buildings of Riyadh, Saudi Arabia; *Results in Physics,* 7: 1792-1798.

International Association of Oil and Gas Producers (IOGP) (2016). Managing Naturally occurring radioactive material in the oil and gas industry. Report 412, March 2016.

Lamarsh, J.R. and Beratta, A.J. (2001). *Introduction to nuclear Engineering,* 3rd Edition, Prentice Hall.

Lele, R.R. (2002). Radiation in Biotechnology and medicine: Future Trends, *IJNM,* 17(I): 2-12.

Lin, U. T. and Jiang, S.H. (1996). A Dedicated Empirical Formula For gamma-ray buildup factors for a point isotropic source in stratified shields; *Radiat. Phys. Chem.*, Vol.48, No. 4, pp. 389-401.

Madbouly, A.M. and Amal, A. E. (2018). Calculation of gamma and neutron parameters for some concretes materials as radiation shields for nuclear facilities. *IJETED,* 8(3).

Manohara, S.R., Hanagodimath, S.M., Gerward, L. (2010). Energy absorption buildup factors for thermoluminescent dosimetric materials and their tissue equivalent. *Radiation Physics and Chemistry,* 79, 575-582.

Mavi, B. and Akkurt, I. (2015). Investigation of Radiation Absorption Properties of Some India Granites. *Acta Physica Polonica*, Vol. 128 A, No. 2-B.

Mirmazhari, S.S., Entezari, A., Emami, A.M.R. (2017). Determination of mechanical characteristics and radiation attenuation coefficients of heavyweight and normal-weight concretes containing hematite for 70 KeV and 570 KeV gamma-rays. *IJCECEM,* Vol 5(2): 13-23.

Najam, L.A., Hashim, A.K., Ahmed, H.A. and Hassan, I.M. (2016). Study the Attenuation Coefficient of Granite to Use It as Shields against Gamma Ray. Detection, 4, 33-39.

Oche, C. O. (2015). Nuclear safety: The case of Fukushima accident and its effect on the public; Unpublished Thesis, Physics Department, University of Abuja.

Olarinoye, O.I. (2017). Photon Buildup factors for some tissues and phantom materials for penetration depths up to 100mfp; *Journal of Nuclear Research and Development,* No. 13.

Olarinoye, O.I., Odiaga, R.I., Paul, S. (2019). EXABCal: A program for calculating photon exposure and energy absorption buildup factors; *Heliyon 5 e02017.*

Olukotun, S.F., Gbenu, S.T., Ibitoye, F.I., Oladejo, O.F., Shittu, H.O., Fasasi, M.K., Balogun, F.A. (2018). Investigation of gamma radiation shielding capability of two clay materials; *Nuclear Engineering and Technology*, xxx 1e6.

Rajavikraman, R. S. (2013). Novel Method for Radiation Shielding Using Nano-Concrete Composite. *International Journal of Materials Science and Engineering,* Vol. 1, No. 1, pp. 20-23.

Ripan, B., Hossaini, S., Mollah, A.S. (2015). Calculation of gamma ray attenuation parameters for locally developed shielding materials: Polyboron, *JRRAS* (9): 26-34.

Sayyed, M. I. (2017). Investigation of shielding parameters of smart polymers, *Chin. J. Phys.* 54, pp. 408-415.

Tejbir, S., Gurpreet, K. and Parjit, S. S. (2013). Study of Gamma Ray Exposure Buildup Factor for Some Ceramics with Photon Energy, Penetration Depth and Chemical Composition; *Journal of Ceramics,* Volume 2013.

Tekin, H. O., Erguzel, T. T., Sayyed, M.I., Singh, V. P., Manici, T., Altunsoy, E. E., Agar, O. (2018). An Investigation On Shielding Properties Of Different Granite Samples Using MCNPX Code Digest. *Journal of Nanomaterials and Biostructures,* Vol. 13, No. 2, pp. 381-389.